example if a steady-state solution is first computed and the unsteady pressure distribution is related by a small perturbation to the steady-state result. Hence, if a modified small disturbance equation has been derived for the steady-state case it may be possible to use a simple analytic perturbation of the function $f(\phi_x)$ that will give good accuracy in the neighborhood of the steady-state result. The additional condition for this idea is given subsequently.

For the shock strength to be approximately correct over a range of values close to the steady-state value $\phi^+_{x_s}$, Eq. (13) can be expanded as a Taylor series to give

$$F(\phi^+_{x_s},\sigma_{E_s}) + \left[\left(\frac{\partial F}{\partial \phi^+_x}\right) + \frac{\partial F}{\partial \sigma_E}\frac{d\sigma_E}{d\phi^+_x}\right]_s (\phi^+_x - \phi^+_{x_s}) = 0 \quad (14)$$

where the subscript s denotes a value in the steady state.

Now, by definition

$$F(\phi^+_{x_s},\sigma_{E_s}) = 0 \quad (15)$$

and, hence, for Eq. (14) to be satisfied for a range of $(\phi^+_x - \phi^+_{x_s})$

$$\frac{\partial F}{\partial \phi^+_x} + \frac{\partial F}{\partial \sigma_E}\frac{d\sigma_E}{d\phi^+_{x_s}} = 0 \quad (16)$$

Thus, our method consists of satisfying Eqs. (11), (12), and (15) at each iterative step in the steady calculations and Eqs. (11), (12), and (16) at each time step in the unsteady calculation.

It is possible to derive functions $f(\phi_x)$ that satisfy all of the conditions given in the preceding section, but in a limited study, such as the present one, it is more convenient to satisfy only certain of these conditions explicitly and to test the resulting function with respect to the other conditions.

The most crucial conditions to satisfy are the shock strength conditions, Eqs. (15) and (16), since the object of the present exercise is to realize the correct shock strengths. Consequently, these conditions are satisfied explicitly. For simplicity in derivation, it is assumed that the modifications to the small disturbance equation will be sufficiently small that Eqs. (11) and (12), at least, will be approximately satisfied.

The form of $f(\phi_x)$ chosen is

$$f(\phi_x) = 1 - M^2_\infty + (\gamma+1)M^2_\infty (\phi^+_x/\phi^+_{x_s})^\alpha \phi_x + \epsilon\phi^2_x \quad (17)$$

Since powers of ϕ_x greater than two are neglected in the derivation of the small disturbance equation the term $\epsilon\phi^2_x\phi_{xx}$ is formally negligible. The exponent α is set equal to 1 during the steady iteration ($\phi^+_x = \phi^+_{x_s}$) and ϵ is chosen to give the steady shock jump relation, Eq. (15). During the unsteady iteration, the value of ϵ is fixed, and the exponent α is adjusted to satisfy the unsteady shock jump condition, Eq. (16), at the upper airfoil surface. The same value of α is used at all points of the flowfield during the next time step. The conservation form of the LTRAN2 algorithm is left unchanged.

Results

In Fig. 1 the unsteady pressures for a NACA 64A410 airfoil at $M_\infty = 0.72$ oscillating in the angle of attack according to $\alpha = 2$ deg $+ 2$ deg $\sin(\omega t)$, $k = 0.2$, are shown at the extremes of oscillation. In these results $q = 1.69$ in Eq. (1). It can be seen that the present method predicts a shock position about 6% chord further forward than the Euler solution.[3] This discrepancy is constant throughout the motion. However, the amplitude and phase of the unsteady shock motion are in good agreement. It is likely that the constant discrepancy can be attributed to differences in the mesh and in the numerical algorithm for the two calculations. In particular, the mesh size affects the shock capturing properties of the algorithm. In this calculation the parameter α is computed to be -0.385 and the constant ϵ is 0.083. It should be noted that a converged solution could not be obtained for this case with the standard TSD equation.

Conclusions

A procedure to correct the transonic small disturbance equation to treat strong shock waves in unsteady flow has been developed. A simplified form of this procedure has been implemented computationally. The comparisons of results of the present method with solutions of the Euler equations are adequate as regards the shock location, and good as regards the unsteady shock motion, although the pressure distribution near the leading edge is not satisfactory. The discrepancy may be due to differences in the respective meshes and in the numerical schemes. This tends to confirm the hypothesis that the error in shock location is due to the error in shock strength. Finally, although the present method gives a considerable improvement over the conventional TSD theory, it is desirable to test the present modification further in order to evaluate the technique fully.

References

[1] Murman, E. and Krupp, J. A., "Computation of Transonic Flows Past Lifting Airfoils and Slender Bodies," *AIAA Journal,* Vol. 10, July 1972, pp. 880-886.

[2] Jameson, A., "Transonic Potential Flow Calculations Using Conservation Form," *Proceedings of the AIAA 2nd Computational Fluid Dynamics Conference,* 1975, pp. 148-161.

[3] Magnus, R. and Yoshihara, H., "Calculations of Transonic Flow Over an Oscillating Airfoil," *AIAA Journal,* Vol. 13, Dec. 1975, pp. 1622-1628.

[4] Nixon, D., "Transonic Small Disturbance Theory with Strong Shock Waves," *AIAA Journal,* Vol. 18, June 1980, pp. 717-718.

[5] Klopfer, G. H. and Nixon, D., "Non-Isentropic Potential Formulation for Transonic Flows," AIAA Paper 83-0375, Reno, Nev., Jan. 1983.

[6] Ballhaus, W. F. and Goorjian, P. M., "Implicit Finite Difference Computations of Unsteady Transonic Flows about Airfoils Including the Effects of Irregular Shock Motions," *AIAA Journal,* Vol. 15, Dec. 1977, pp. 1728-1735.

[7] Liepmann, H. and Roshko, A., *Elements of Gas Dynamics,* Wiley, New York, 1957.

[8] Kerlick, G. D., Nixon, D., and Ballhaus, W. F., "Unsteady Transonic Small Disturbance Theory with Strong Shock Waves," AIAA Paper 82-0159, Orlando, Fla., Jan. 1982.

Effects of Artificial Excitation upon a Low Reynolds Number Mach 2.5 Jet

G. L. Morrison*
Texas A&M University, College Station, Texas

Introduction

THE existence of coherent structures in axisymmetric jets has been under investigation for many years. Mollo-Christensen[1] first observed coherent structures in jets by the use of space-time cross correlations in the near acoustic field. Many others have pursued the subject in a similar manner by using two probes (hot-wires, microphones, etc.) and space-time cross correlations to help identify the nature of the

Presented as Paper 81-2010 at the AIAA 7th Aeroacoustics Conference, Palo Alto, Calif., Oct. 5-7, 1981; submitted Oct. 16, 1981; revision received Sept. 24, 1982.

*Associate Professor of Mechanical Engineering. Member AIAA.

structure in the flow. Some investigators opted to excite the flow artificially and measure the flow's response to the excitation. In this manner, one probe was eliminated and the exciter signal was used as a time reference for the cross correlation or for phase averaging the probe output. Ideally, if the excitation is small enough, the jet will remain unaltered due to the excitation and the results should agree with those obtained in an unexcited jet using two probes.

For a jet with a Mach number less than 0.1, Crow and Champagne[2] used a loud speaker excitation device in order to measure the wave properties of the coherent structure present in the jet. Moore,[3] continuing the work, showed that it was possible to use excessive levels of excitation in subsonic jets which resulted in a substantially altered flowfield. Therefore, the effects of the excitation upon the acoustic and flowfields should be investigated any time a jet is excited artificially.

Morrison and McLaughlin[4,5] investigated the present low Reynolds number (8700), Mach 2.5, axisymmetric, cold air jet in order to determine the manner in which noise was radiated by the large-scale coherent structure present in the jet. This low Reynolds number jet was used since the flow was undergoing transition from laminar to turbulent flow. At this Reynolds number, the flow possessed an instability that was characterized as a classical instability. This enabled us to study the organized structure much more easily than in a high Reynolds number jet. In order to accomplish the characterization of the organized structure, it was necessary to artificially excite the jet to provide the phase reference needed for conditionally sampling the jet. The organized structure in the jet "locked" onto the exciter signal and amplified that signal as it would normally amplify the random fluctuations convected through the nozzle. This paper will direct its attention to the effects of that artificial excitation upon the flow and acoustic fields of the jet.

Experimental Apparatus and Procedures

The low Reynolds number jet was obtained by exhausting the jet into an anechoic vacuum chamber. The vacuum chamber was maintained at a pressure of 0.0073 atm (P_c). The facility layout and support equipment have been described previously by Morrison and McLaughlin.[4,5]

The excitation device used was a glow discharge similar to the one used by Kendall.[6] In these experiments, a 1.6-mm diameter, 2% thoriated tungsten electrode was embedded in the wall of the converging-diverging nozzle ($D=6.86$ mm) about 2 mm from the exit. The electrode was insulated from the aluminum nozzle by a ceramic sleeve. The nozzle was grounded and a 135 V peak to peak ac signal biased to -415 V dc was applied to the electrode. The frequency of the ac component was varied so that a disturbance with the desired frequency could be introduced.

The flow was measured using hot-wire anemometry. For this flowfield, the hot-wire voltage was proportional to the axial mass flux. The acoustic measurements were performed with a B&K 3.175-mm diameter microphone. The sound pressure levels presented in this paper were calculated using a reference pressure scaled to the ambient pressures in the test facility: $P_{\text{ref}} = (2\times10^{-5})(P_c/1\text{ atm})$.

Experimental Results

Spectra of the flow fluctuations measured at the radial location of maximum fluctuation level contained several different discrete frequency components (Fig. 1). As the flow progressed downstream, the dominant spectral component varied from $St=0.13$ to 0.16 and the spectrum became broader due to the effects of random turbulence. Measurements in the radial direction showed that in this Strouhal number range, all frequencies attained their maximum fluctuation level at approximately the same radial location. It was only at substantially higher frequencies that any other radial dependence became evident. However, these higher frequencies were not important in the generation of the noise.[5] At $X/d=16$, the discrete peaks attained their maximum amplitude and then began to decay. This was also the location where the potential core ended and the coherence of the organized structure began to decay quite rapidly.[4,5] Of the discrete peaks that appeared in the spectra, only the $St=0.16$ component remained in the jet from $X/d=1$ to 20. Therefore, it was the frequency selected from which to study the effects of artificial excitation upon the jet.

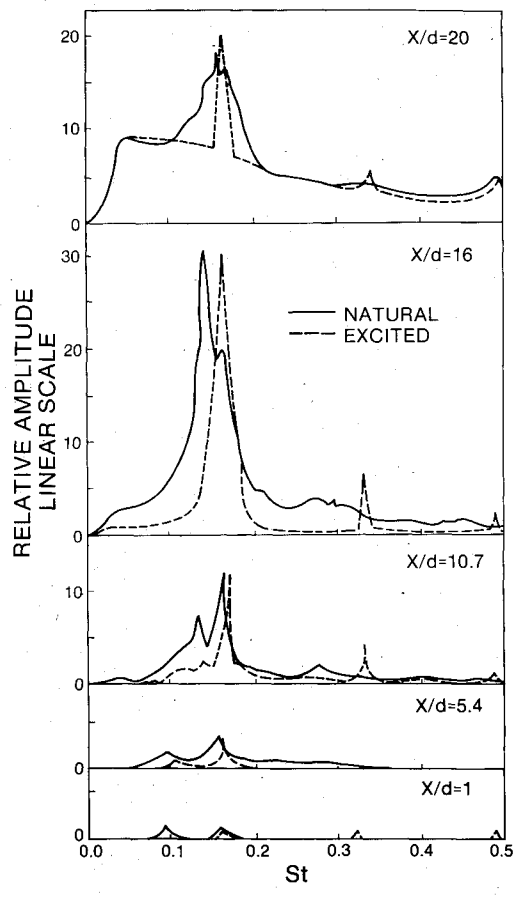

Fig. 1 Flow fluctuation spectra, natural and excited at $St=0.16$. (d = effective inviscid diameter $=D/1.12$).

Figure 1 also shows spectra recorded at the same locations as the spectra in Fig. 1 when the jet was artificially excited. The excitation caused the jet to stabilize onto the exciter frequency and the broadband turbulence decreased at the locations upstream of the end of the potential core. Further downstream the broadband turbulence level remained about the same. When the jet was excited, a disturbance with constant amplitude, frequency, and phase reference was present for amplification. Before the jet was excited, the signal available for amplification was only the naturally occurring, random fluctuations convected through the nozzle from upstream. Thus, in the unexcited jet, a broadening of the spectral peaks due to shifts in the frequency content of the random fluctuations about the frequency range of maximum amplification occurred. This broadening effect is well illustrated in the spectra recorded at $X/d=20$.

In addition to the stabilizing of the fundamental frequency onto the exciter frequency, there was an increase in the harmonic content of the jet. This increase in harmonic content could be caused by one of two different phenomena. The first possibility is that the excitation caused nonlinear interactions to occur closer to the jet exit and, hence, reinforce the harmonics much sooner than in the unexcited jet.

The second possibility is that there was no nonlinear interaction between the fundamental frequency and the harmonics. The spectrum recorded at $X/d=1$ shows that the artificial exciter input disturbances at not only the fun-

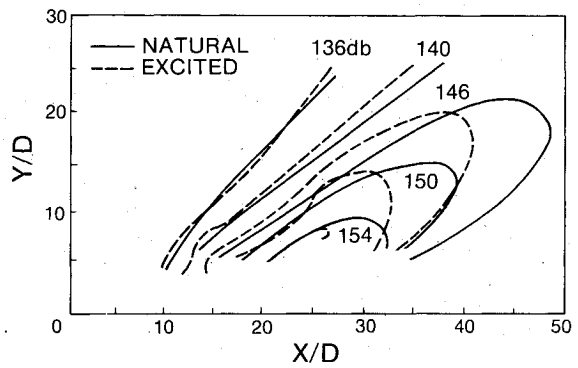

a) Low level excitation.

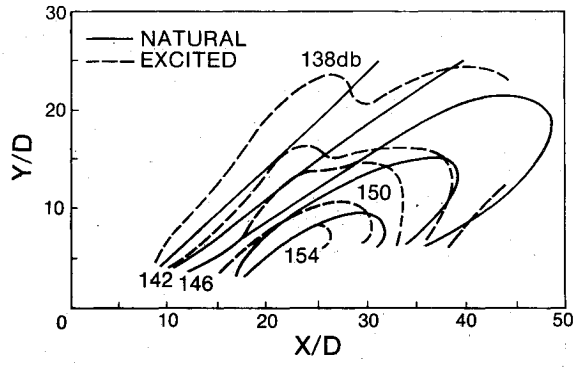

b) High level excitation.

Fig. 2 Sound pressure level contours, natural and excited at $St = 0.16$.

damental frequency, but at its harmonics as well. This was due to the fact that the exciter produced a glow discharge that pulsed on and off. Morrison[7] further showed that for $X/d < 15$ that the fundamental frequency and its harmonic both increased in amplitude exponentially as they progressed downstream. Miksad[8] observed in a subsonic wake that nonlinear interactions between the fundamental and first harmonic occurred when the fundamental frequency stopped growing exponentially in amplitude and began diverting its energy to the harmonic. Since both the fundamental and first harmonic component grew exponentially over the same region of the jet, it is apparent that it was a linear phenomenon due to the input of the harmonic into the jet shear layer by the excitation device.

Profiles of the mean and rms values of the hot-wire voltage at several axial locations were measured when the jet was excited and unexcited. The overall characteristics of both sets of profiles were uneffected by the excitation of the jet. The only difference was that the potential core of the jet was slightly shorter when the jet was excited which resulted in a compacting, in the axial direction, of the flowfield's development.

The faster decay of the mean flow when the jet was excited can be explained by examining the axial distributions of the flow fluctuation's amplitude. When the jet was excited, the initial level of fluctuation at the jet exit was increased above the level in the natural jet. In both cases, the fluctuation level initially increased exponentially at the same rate[4] as the flow progressed downstream and eventually attained the same maximum level. Thus, the flow fluctuations were extracting energy from the mean flow more rapidly when the jet was excited and, hence, slightly shortened the length of the potential core. Since the excitation did not alter the growth rate, the mechanism by which the disturbances were amplified did not seem to be altered by the excitation.

Comparisons of the spectra in Fig. 1 with these fluctuation amplitude distributions yield some interesting observations. At $X/d = 5.4$, the mass velocity fluctuation level was larger in the excited jet. From the spectra we can see that this increase was not due to the enhancement of the fundamental frequency ($St = 0.16$) by the excitation. In fact, the excitation decreased the power contained in the spectrum for the Strouhal number range of 0.1-0.2. The increase in fluctuation level was due to the added presence of the harmonics. As the flow progressed downstream, the fluctuation amplitudes were approximately equal at $X/d = 10.7$ and the unexcited jet possessed slightly higher fluctuation levels at $X/d = 16$. In both cases, the excitation decreased the broadband random turbulence, narrowed the breadth of the peak at the fundamental frequency, and enhanced the harmonics.

All of the preceding measurements show that there was only a moderate change in the flowfield when the jet was excited. However, it was discovered that the acoustic field was more sensitive to the effects of excitation than the flow itself. Sound pressure level (SPL) contours were measured in the acoustic field of the jet when the jet was in its natural condition and when it was excited at two different intensity levels at $St = 0.16$. These SPL contours are shown in Fig. 2. The SPL contours for the unexcited jet were similar to those measured by other investigators for high Reynolds number jets.[9] When the exciter mechanism was adjusted such that the dc bias was drawing approximately 2.0 mA of current, the shape of the SPL contours were changed substantially (Fig. 2b). A spurious lobe was added to the SPL contours while the maximum amplitude of the pressure fluctuations at $Y/D = 25$ decreased. The ratio of the power input into the exciter mechanism to the power of the jet (kinetic energy flux) was 0.0156. By lowering the level of excitation such that this ratio was 0.0048, there was a smaller difference in the SPL contours. At a given radial distance from the jet, the amplitude of the SPL contours decreased slightly while the shape of the contours remained essentially the same with only a moderate shift upstream.

The decrease in SPL can be explained by referring back to the discussion of the mass velocity fluctuation levels and the spectra. The majority of the noise radiated by the jet originated in the axial region[5] from $X/d = 13$ to 20. In this region, the overall fluctuation level for the natural and excited jets was about the same.[4] However, the excited jet contained less broadband noise and more harmonics as shown in Fig. 1. It appears that these higher frequencies are less efficient noise radiators since the overall SPL levels dropped. Ahuja et al.[10] studied the effects of pure tone acoustic excitation upon fully turbulent jets. They found that the jet responded more (produced more noise) when excited in a mid range of frequencies and that at some lower frequencies (St around 0.1) the overall SPL could even decrease, as was seen here. The upstream shifting of the SPL contours was due to the upstream compacting of the development of the mean flow when the jet was excited. For all of the previous portions of this paper when the jet was excited and the flow fluctuations were measured, the lower level of excitation was used.

Acknowledgments

This research was supported by the National Science Foundation under Grant ENG 75-21405 and by NASA under Grant NSG 1467. The author takes pleasure in acknowledging the assistance and suggestions of D.K. McLaughlin, W.G. Tiederman, J.L. Stromberg, and T.R. Troutt.

References

[1] Mollo-Christensen, E., "Jet Noise and Shear Flow Instability Seen from an Experimenter's Viewpoint," *Journal of Applied Mechanics*, Vol. 34, March 1967, pp. 1-7.

[2] Crow, S.C. and Champagne, F.H., "Orderly Structure in Jet Turbulence," *Journal of Fluid Mechanics*, Vol. 48, Aug. 1971, pp. 547-591.

[3]Moore, C.J., "The Role of Shear Layer Instability Waves in Jet Exhaust Noise," *Journal of Fluid Mechanics,* Vol. 80, April 1977, pp. 321-367.
[4]Morrison, G.L. and McLaughlin, D.K., "The Instability Process in Low Reynolds Number Supersonic Jets," *AIAA Journal,* Vol. 18, July 1980, pp. 793-800.
[5]Morrison, G.L. and McLaughlin, D.K., "The Noise Generated by Instabilities in Low Reynolds Number Supersonic Jets," *Journal of Sound and Vibration,* Vol. 65, July 1979, pp. 177-191.
[6]Kendall, J.M., "Supersonic Boundary Layer Stability Experiments," *Proceedings of the Boundary Layer Transition Study Group Meeting,* Vol. II, Aerospace Rept. TR-0158 (S3816-63)-1, 1967.
[7]Morrison, G.L., "Flow Instability and Acoustic Measurements on Low Reynolds Number Supersonic Jets," Ph.D. Dissertation, Oklahoma State University, 1977.
[8]Miksad, R.W., "Experiments on the Non-Linear Stages of Free Shear-Layer Transition," *Journal of Fluid Mechanics,* Vol. 56, Dec. 1972, pp. 695-719.
[9]McLaughlin, D.K., Morrison, G.L., and Troutt, T.R., "Reynolds Number Dependence in Supersonic Jet Noise," *AIAA Journal,* Vol. 15, April 1977, pp. 526-532.
[10]Ahuja, K.K., Lepicovsky, J., and Burrin, R.H., "Acoustic and Turbulence Measurements of a Tone Excited Jet With and Without Flight Simulation," AIAA Paper 81-2007, 1981.

Analytical Approximation of Two-Dimensional Separated Turbulent Boundary-Layer Velocity Profiles

T. W. Swafford*
Sverdrup Technology, Inc.
Arnold Air Force Station, Tennessee

Introduction

THE calculation of separated two-dimensional flow using an inverse formulation of the boundary-layer equations[1-6] is attractive because of simplicity and cost reduction compared to solving the Navier-Stokes equations, providing that solution of the boundary-layer equations yields acceptable engineering accuracy. These computation methods can be classed as either integral or differential. Most integral methods require an analytical description of the boundary-layer velocity profile[1,3,6] such that the integral quantities can be evaluated. The purpose of this Note is to present an analytical representation of two-dimensional turbulent boundary-layer velocity profiles that describes attached and separated flow over the entire domain $0 \le y < \infty$. (This analytic representation was reported earlier,[6] but attention here is focused on the details of the development.) The derivation of this expression is presented and examples given to illustrate the quality of agreement with experimental data. Profile correlations resulting from empirical fits of this expression to measured data are also presented. These correlations, along with the velocity profile representation, allow separated turbulent boundary-layer velocity profiles to be generated as a function of shape factor and momentum thickness Reynolds number. Steps to applying the velocity profile expression are summarized in Table 1.

Received July 12, 1982; revision received Oct. 25, 1982.

*Research Engineer, Computational Fluid Dynamics, AEDC Group. Member AIAA.

Analytical Development

The equation proposed to describe reversed flow velocity profiles on smooth, impermeable, adiabatic walls in incompressible flow is an extension of the expression derived by Whitfield,[7] which is a composite function of the form

$$u^+ = u_i^+ + u_o^+ \tag{1}$$

consisting of an inner expression (u_i^+) originally presented in Ref. 8 and an outer expression (u_o^+) derived in Ref. 7. The inner solution as presented in Ref. 7 is given by

$$u_i^+ = (1/0.09)\tan^{-1}(0.09y^+) \tag{2}$$

where

$$u_i^+ = u_i/u_\tau \qquad y^+ = u_\tau y/\nu \qquad u_\tau = (c_f/2)^{1/2} u_e \tag{3}$$

Assumptions made in deriving Eq. (2) for attached flow[8] are also made herein to retain the form of Eq. (2).

The velocity profile slope at the wall, computed from Eq. (2), is positive for attached flow. A negative slope for separated flow can be obtained by simply taking the negative of Eq. (2) and redefining u_τ as $u_\tau = (|c_f|/2)^{1/2} u_e$. Thus, for u^+ to have the correct value of u_e^+ as $y \to \infty$, u_o^+ must behave as

$$u_o^+ \to \left[u_e^+ - \left(-\frac{\pi}{0.18}\right)\right] \tag{4}$$

as $y \to \infty$. In addition, because u_i^+ behaves correctly near the wall, u_o^+ must approach zero as y approaches zero. Therefore the form considered in Ref. 7,

$$u_o^+ = \left[u_e^+ - \left(-\frac{\pi}{0.18}\right)\right] g\left(\frac{y}{\theta}\right) \tag{5}$$

is retained, where $g(y/\theta)$ has the values of $g(0) = 0$ and $g(\infty) = 1$.

In Ref. 7, the form of $g(y/\theta)$ which gave the best overall fit of measured data was determined to be

$$g\left(\frac{y}{\theta}\right) = \tanh^{1/2}\left[a\left(\frac{y}{\theta}\right)^b\right] \tag{6}$$

where a and b are parameters that are functions of c_f, H, and Re_θ (H is the usual boundary-layer shape factor). It should be emphasized that the parameters a and b are different for each velocity profile. This same functional form of $g(y/\theta)$ is retained in the present work. Therefore the proposed analytical representation of two-dimensional incompressible, attached and separated, turbulent boundary-layer velocity profiles becomes

$$u^+ = \frac{s}{0.09}\tan^{-1}(0.09y^+) + \left(u_e^+ - \frac{s\pi}{0.18}\right)\tanh^{1/2}\left[a\left(\frac{y}{\theta}\right)^b\right] \tag{7}$$

where

$$u_e^+ = \left(\frac{2}{|c_f|}\right)^{1/2} \qquad y^+ = \frac{Re_\theta}{u_e^+}\frac{y}{\theta} \qquad \frac{u}{u_e} = \frac{u^+}{u_e^+} \qquad s = \frac{c_f}{|c_f|} \tag{8}$$

Equation (7) can be rearranged to give the velocity ratio u/u_e as a function of physical distance y, local unit Reynolds number, and local skin friction. Therefore, given u/u_e at three points in the boundary layer, a system of three equations [Eq. (7) at each point] and three unknowns (u_e^+, a, and b) is obtained. The velocity measurements of Simpson[9] and Alber